

Microsecond Electro-Optic Switching of Nematic Liquid Crystals with Giant Dielectric Anisotropy

Bing-Xiang Li^{1,2,*}, Greta Babakhanova,^{1,2} Rui-Lin Xiao,^{1,2} Volodymyr Borshch,^{1,2}
Simon Siemianowski,³ Sergij V. Shiyanovskii,^{1,2} and Oleg D. Lavrentovich^{1,2,4,†}

¹*Advanced Materials and Liquid Crystal Institute, Kent State University, Kent, Ohio 44242, USA*

²*Chemical Physics Interdisciplinary Program, Kent State University, Kent, Ohio 44242, USA*

³*Merck KGaA, Darmstadt, Germany, 64293, Germany*

⁴*Department of Physics, Kent State University, Kent, Ohio 44242, USA*



(Received 6 March 2019; revised manuscript received 18 July 2019; published 2 August 2019)

Nematic liquid crystals exhibit a fast optical response when the applied electric field modifies the degree of order but does not change the direction of molecular orientation. The effect requires a relatively high electric field, on the order of 10^8 V/m for a field-induced birefringence change of 0.01. To address this detrimental issue, we explore electrically induced modification of the order parameter in a material with a giant dielectric anisotropy of +200. A relatively weak field of 3×10^7 V/m causes a significant change of birefringence of about 0.04. Both switching on and off times are approximately $10 \mu\text{s}$. The effect is called a microsecond electrically modified order parameter effect and can be used in electro-optical devices, such as fast electro-optic shutters, phase modulators, and beamsteerers that require microsecond response times.

DOI: [10.1103/PhysRevApplied.12.024005](https://doi.org/10.1103/PhysRevApplied.12.024005)

I. INTRODUCTION

Nematic liquid crystals (NLCs) are used extensively in electro-optic applications because of their anisotropic dielectric and optical properties [1–3]. The average orientation direction of NLC molecules, called a director $\hat{\mathbf{n}}$, is also the optic axis. Most of the electro-optical applications of NLCs exploit the so-called Frederiks transition [4], that is, reorientation of $\hat{\mathbf{n}}$ by an external electric field followed by elastic relaxation of $\hat{\mathbf{n}}$ when the field is switched off. The latter process is very slow as the driving force is a surface anchoring of $\hat{\mathbf{n}}$ at the bounding plates. The time of director reorientation is determined by the ratio of the viscous and elastic coefficients of the NLC, which yields a response time on the scale of milliseconds and above. Many research groups have explored ways to reduce the switching time to the millisecond or submillisecond range by optimizing the dielectric and viscoelastic parameter of NLCs, using dual frequency NLCs [5–7], introducing polymer-layer-free alignment [8], and designing the spatial configuration of electric fields [9]. Still, the response time of the typical nematic based electro-optic devices in which the electric field realigns the director $\hat{\mathbf{n}}$ rarely reaches the scale of $100 \mu\text{s}$ or less.

Recently, an alternative approach to electro-optic switching of NLCs has been proposed [10–12]. In

this approach, the electric field modifies the degree of molecular order but does not realign $\hat{\mathbf{n}}$. The effect, called the nanosecond electrically modified order parameter (NEMOP), has been demonstrated for NLCs with a negative dielectric anisotropy [10–12]. In these materials, with a typical $\Delta\epsilon \approx -10$, the field-induced birefringence, δn , is about 0.02 for an applied electric field on the order of 10^8 V/m, while the switching speed is tens of nanoseconds. The current challenge is to reduce the driving field as compared to the NEMOP effect, while enhancing the birefringence change and making the response time significantly shorter than in the conventional Frederiks effect. In this work, we demonstrate that by using an NLC composition abbreviated as GPDA200 (Merck KGaA), with a giant positive dielectric anisotropy (GPDA), $\Delta\epsilon > +200$, one can achieve a significant birefringence change of 0.04 at the applied field of 3×10^7 V/m with switching times on the order of $10 \mu\text{s}$ for both field-on and -off switching. We call the effect a microsecond electrically modified order parameter or MEMOP effect.

II. MATERIALS AND METHODS

A. Dielectric and optical properties of the NLC

To measure the birefringence of the mixture GPDA200, we place a planar cell of thickness $d = 10.8 \mu\text{m}$ between two crossed polarizers in such a way that the rubbing direction of the cell is at an angle of 45° with respect to the polarizers. An ac voltage is applied using transparent

*bli15@kent.edu

†olavrent@kent.edu

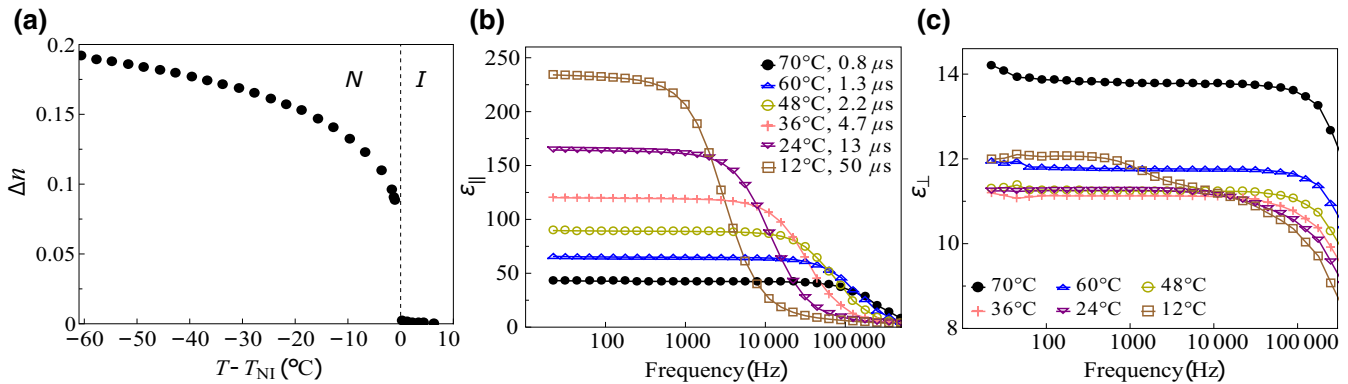


FIG. 1. Material parameters of GPDA200. (a) Temperature dependency of the birefringence at $\lambda = 632.8$ nm. (b) Frequency dependencies of $\varepsilon_{||}$ at various temperatures in the nematic phase and the corresponding Debye relaxation times. (c) ε_{\perp} as a function of frequency at different temperatures in the nematic phase.

indium tin oxide (ITO) electrodes at the glass bounding plates of the cell in order to cause reorientation of \hat{n} toward the field direction. The birefringence Δn , measured with a probing beam of a He-Ne laser of wavelength $\lambda = 632.8$ nm, is calculated from the field dependency of the transmitted intensity

$$\Delta n = \frac{\lambda}{2d} \left(j + \frac{1}{2} + \frac{(-1)^j}{\pi} \arcsin \frac{2I - I_{\max} - I_{\min}}{I_{\max} - I_{\min}} \right), \quad (1)$$

where j shows how many times the transmitted light intensity oscillates between the maximum intensity I_{\max} and the minimum intensity I_{\min} and I is the transmitted intensity in the absence of the field, Fig. 1(a). For dielectric measurements, we use an LCR meter (HP4284A) and homemade cells of thicknesses $d = 19.1 - 19.9 \mu\text{m}$ with planar and homeotropic anchoring. The planar alignment is achieved with antiparallel rubbed PI2555 polyimide layers (HD Microsystems), while the homeotropic alignment is realized using an SE1211 polyimide layer (Nissan Chemical Industries). The dielectric permittivity $\varepsilon_{||}$ along \hat{n} is huge and highly dependent on both the temperature and field frequency, following the Debye model with a single relaxation time τ_D , Fig. 1(b). In contrast, the perpendicular component ε_{\perp} is small, Fig. 1(c). Thus, the dielectric anisotropy $\Delta\varepsilon = \varepsilon_{||} - \varepsilon_{\perp}$ is positive. It also fits the Debye model with the same τ_D well. Upon cooling, both τ_D and the low-frequency $\Delta\varepsilon$ increase dramatically.

B. Experimental setup and method of electro-optic switching of NLC

To trigger the MEMOP effect in a material with $\Delta\varepsilon > 0$, the electric field should be applied parallel to the director $\hat{n} = (n_x, n_y, n_z) = (0, 0, 1)$, which implies using a homeotropic cell. To maximize the field-induced birefringence, the light should propagate under some angle to the

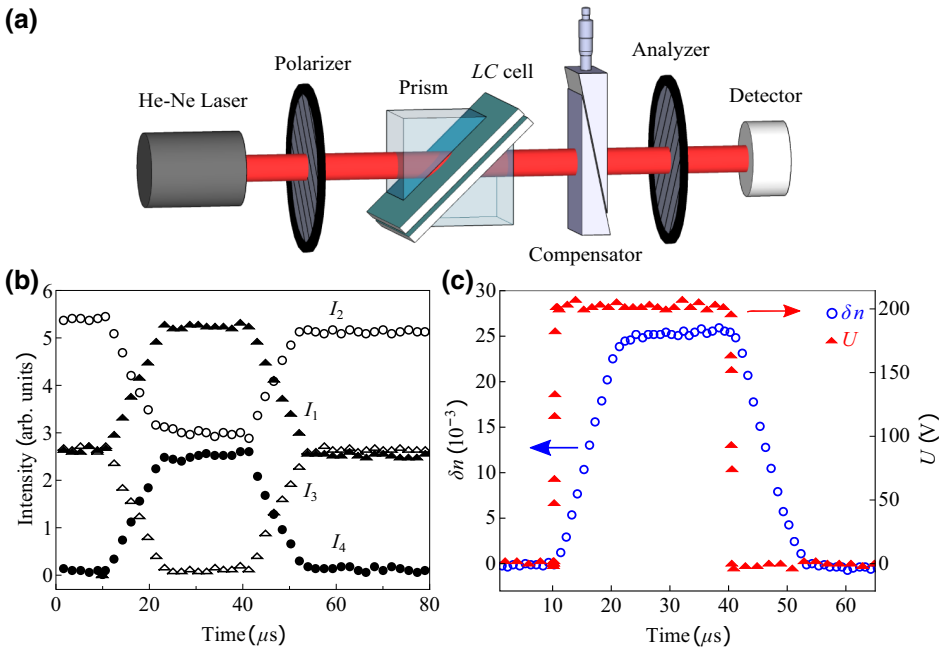
electric field. We choose the angle close to 45° by sandwiching the flat cell between two 45° prisms, Fig. 2(a). The homeotropic cell is composed of two parallel glass substrates with ITO electrodes of low resistivity ($10 \Omega/\square$) and a polyimide alignment layer SE1211. The area of the electrodes is $2 \times 2 \text{ mm}^2$ and the cell thickness is in the range of 4.4 to $7.0 \mu\text{m}$.

A laser beam (He-Ne, $\lambda = 632.8$ nm) passes through the polarizer (P), LC cell, Soleil-Babinet compensator, and the analyzer (A) with the polarization direction being perpendicular to that of the polarizer, $A \perp P$. The transmitted light intensity is determined by using a photodetector TIA-525 (Terahertz Technologies) with a response time < 1 ns. The director \hat{n} makes a projection onto the plane formed by P and A ; this projection makes an angle of 45° with both P and A . A dc voltage pulse with a duration of $30 \mu\text{s}$ is applied using a waveform generator, Model 3390 (Keithley) and amplified by a wideband amplifier, Model 7602 (Krohn-Hite). The applied voltage pulses and photodetector signals are measured with a 1G sample/s digital oscilloscope TDS2014 (Tektronix).

In order to measure the field-induced optical retardance $\delta\Gamma(t)$ and the corresponding effective birefringence $\delta n = \delta\Gamma(t)/d$, we use the four-point measurement scheme [13]. The technique is based on four successive measurements of the transmitted intensities I_k , ($k = 1, 2, 3, 4$) subjected to an identical electrical pulse at four different settings of the Soleil-Babinet compensator Γ_k^{SB}

$$I_k(t) = [I_{\max}(t) - I_{\min}(t)] \sin^2 \left\{ \frac{\pi}{\lambda} \Gamma_k(t) \right\} + I_{\min}(t), \quad (2)$$

where $\Gamma_k(t) = \Gamma_{LC}(0) + \Gamma_k^{\text{SB}} + \delta\Gamma(t)$ is the total dynamic optical retardance of the system and $\Gamma_{LC}(0)$ is the optical retardance of the LC cell when no electric field is applied. We select $\Gamma_k^{\text{SB}} = \lambda(m + k/4) - \Gamma_{LC}(0)$, where m is an integer, in such way that the initial intensities with zero field are maximum $I_2(0)$, minimum $I_4(0)$, and



mean $I_1(0) = I_3(0) = [I_2(0) + I_4(0)]/2$ values, Fig. 2(b), and for this selection, the field-induced birefringence is calculated as

$$\delta n = \frac{\lambda}{2\pi d} \arg\{I_2(t) - I_4(t) + i[I_1(t) - I_3(t)]\} \quad (3)$$

where λ is the wavelength of the laser beam and d is the thickness of the cell, Fig. 2(c). Note that Eq. (3) corrects the misprint in the corresponding equation in Ref. [13]. The switching-on time τ_{on} and the switching-off time τ_{off} are defined as the time when the field-induced birefringence changes between 10% and 90% of its maximum value, respectively.

III. RESULTS AND DISCUSSIONS

We measure the electro-optical responses in the nematic phase in the temperature range of $T = 28^\circ\text{C}$ to 72°C . The microsecond dynamics of δn at various applied electric fields and temperatures is shown in Figs. 3(a) and 3(b). Higher electric fields and temperatures result in higher δn values, Figs. 3(a) and 3(b). The switching times τ_{on} and τ_{off} are on the order of microseconds, Figs. 3(c) and 3(d). The saturation value of δn shows a linear increase with an applied electric field, Fig. 3(e), and an increase with T , Fig. 3(f).

The field-induced birefringence δn in the MEMOP effect in GPDA200 is significant and is achieved at electric fields that are an order of magnitude lower than those reported previously for NEMOP in NLCs with a negative dielectric anisotropy [10–12]. For example, in the previously studied HNG715600-100 ($\Delta\epsilon = -12$, $T = 23^\circ\text{C}$), $\delta n = 0.013$ was achieved under the applied field $E =$

FIG. 2. Experimental methods. (a) Experimental setup. (b) Light intensity dynamics at four different compensator settings. (c) The dynamics of field-induced birefringence δn (circles) calculated from (b) and the corresponding voltage pulse U (triangles).

$170 \text{ V}/\mu\text{m}$ [12], while the same δn in GPDA200 is already achieved at $E = (11\text{--}33) \text{ V}/\mu\text{m}$, depending on the temperature, Fig. 3(e).

The field-induced birefringence in materials with positive dielectric anisotropy is caused by the quenching of the director fluctuations [14] and modification of the uniaxial order parameter [11]. The modification of the uniaxial order parameter is proportional to the square of the field [11]. Quenching of the director fluctuations by the electric field is a well-known phenomenon associated with the anisotropy of liquid crystals. For example, as shown by Dunmur et al, an electric field applied to a nematic with a positive dielectric anisotropy tends to align the director parallel to itself and thus suppresses the director fluctuations [15]. Within the studied range of the applied electric fields, GPDA200 shows that the field-induced birefringence δn grows linearly with the electric field, Fig. 3(e). The linear dependency indicates that the contribution to δn from the director fluctuations quenched by the electric field dominates over the contribution from the enhanced uniaxial order parameter. This result could be explained by the fact that the weaker field (10^7 V/m vs 10^8 V/m) still quenches director fluctuations through a strong dielectric coupling ($\Delta\epsilon = +200$), but at the same time, does not cause a strong modification of the uniaxial order parameter, which indicates a weak uniaxial susceptibility. Using the model [11], we calculate the field-induced birefringence caused by quenching of the director fluctuations in a homeotropic cell as

$$\delta n = \frac{3\delta\tilde{\epsilon}_f}{4\sqrt{2}n_e} \approx \frac{6k_B T \Delta n \sqrt{\epsilon_0 \Delta\epsilon} E}{\sqrt{2} K_{\text{eff}}^{3/2}}, \quad (4)$$

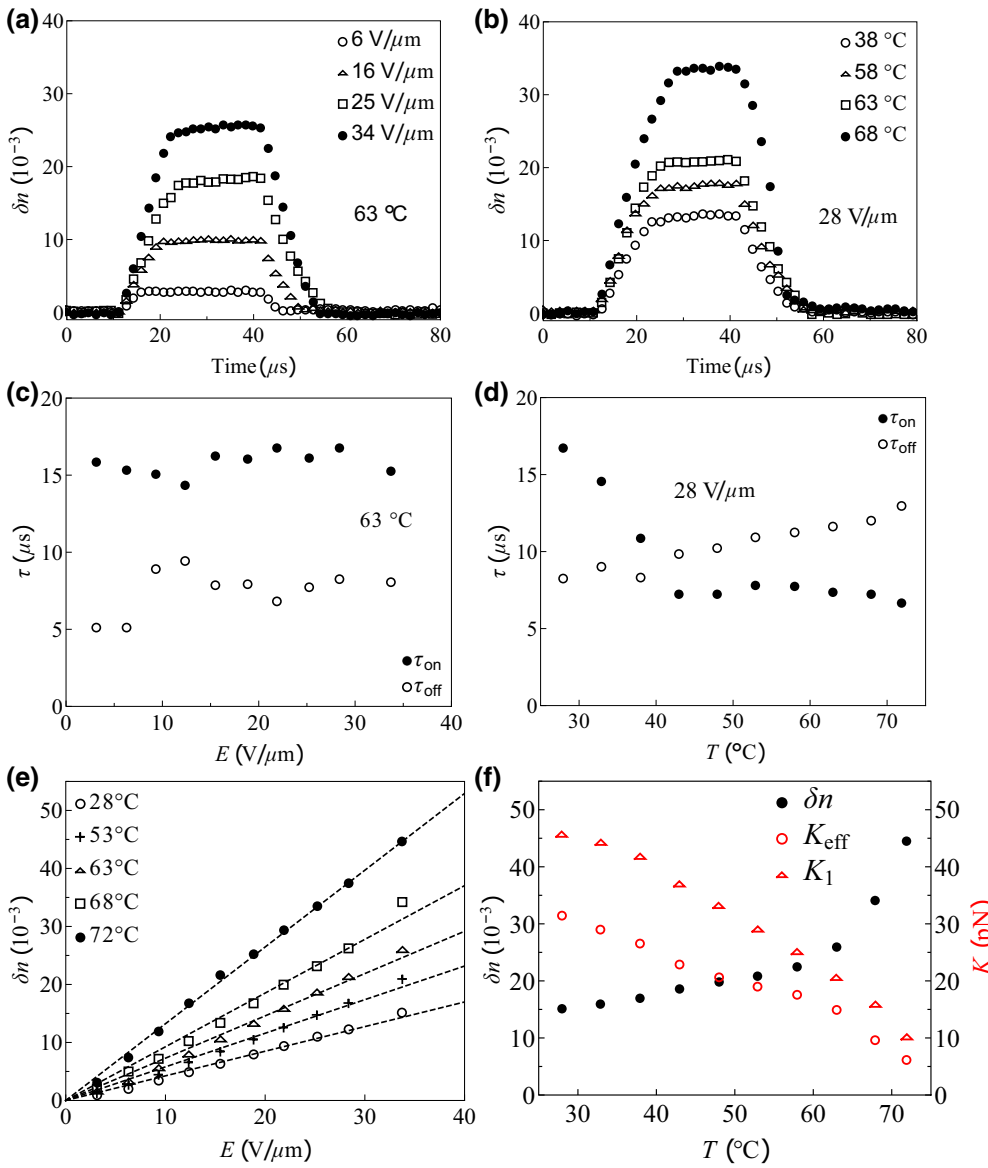


FIG. 3. Microsecond electro-optic switching of GPDA200 at various temperatures and different electric fields. (a) Dynamics of the field-induced birefringence at various electric fields at 63 °C and (b) various temperatures at 28 V/μm. (c) Electric field dependence at 28 °C and (d) temperature dependence at 28 V/μm of the characteristic response time. (e) Maximum value of the field-induced birefringence as a function of an electric field. The dashed lines show the linear fitting. (f) Temperature dependence of δn (34 V/μm), the effective elastic constant K_{eff} , and the splay elastic constant K_1 of GPDA200. K_{eff} is calculated using Eq. (4).

where $\delta\tilde{\epsilon}_f = \langle\tilde{\epsilon}_{zz}(E)\rangle_V - \langle\tilde{\epsilon}_{zz}(0)\rangle_V$ is the field-induced modification of the optic tensor's zz component averaged over the cell volume V , n_e is the extraordinary refractive index of the NLCs, $k_B = 1.38 \times 10^{-23} \text{ J/K}$ is the Boltzmann constant, $\epsilon_0 \approx 8.85 \times 10^{-12} \text{ F/m}$ is the electric constant, and $K_{eff} = (4K_3)^{1/3}(K_1^{-1} + K_2^{-1})^{-2/3}$ is the effective elastic constant, where K_1 , K_2 , and K_3 are the splay, twist, and bend elastic constants of the NLCs, respectively.

It is of interest to compare the linear dependence of δn on the electric field in our work with the field dependence of the induced birefringence $\delta n(E)$ reported by Dunmur, Waterworth, and Palfy-Muhoray for conventional nematics pentylcyanobiphenyl with $\Delta\epsilon = 13$ [15], which is at least 10 times weaker than the $\Delta\epsilon$ of our material. Furthermore, in Ref. [15], the maximum applied electric field was 5 V/μm, which is about one order of magnitude smaller than the fields used in our experiments. Because of these

large differences in the field and dielectric anisotropies, the data of Ref. [15] should be compared to the low end of the field interval in Fig. 3(e). A careful analysis demonstrates that in Ref. [15], the field-induced change of birefringence is, in fact, linear when the field becomes higher than $E_{fluct} = 0.3 \text{ V/μm}$ for a cell of thickness $d = 111 \mu\text{m}$, 0.6 V/μm for $d = 55 \mu\text{m}$, and 2 V/μm for $d = 15 \mu\text{m}$. These linear dependencies are similar to the linear dependencies observed in our work. At lower voltages, the dependence $\delta n(E)$ found in Ref. [15] is not linear and can be approximated as $\delta n(E) \sim E^2$. The reason is that the low fields quench only some of the fluctuations, those with few lowest values of the normal component of the wavevector, $q_z = (\pi/d)m$, where $m = 1, 2, 3, \dots$. As the field becomes stronger, it quenches a larger and larger portion of the fluctuations spectrum and the dependence $\delta n(E)$ becomes linear, as evidenced both by our results in Fig. 3(e) and

by the data in Ref. [15] for fields higher than the E_{fluct} values presented above. Morphing of the dependence $\delta n \propto E^2$ into the linear one as the field increases above E_{fluct} is supported by the thickness dependence $E_{\text{fluct}} = \beta/d\sqrt{\Delta\varepsilon}$, where $\beta \sim 100$ V is a fitting parameter, estimated from the analysis of data presented in Ref. [15]. For our material with $\Delta\varepsilon = 200$ in a cell of thickness $6\ \mu\text{m}$, using the value $\beta \sim 100$ V, we find $E_{\text{fluct}} = \beta/d\sqrt{\Delta\varepsilon}$ to be about $1.2\ \text{V}/\mu\text{m}$, which is smaller than the weakest applied field used in our experiments, see Fig. 3(e). As a result, data shown in Fig. 3(e) correspond to the range where the induced birefringence grows linearly with the electric field.

The fluctuations are expected to grow as one approaches the clearing temperature, Eq. (4). This feature explains why the measured δn increases with temperature, Figs. 3(e) and 3(f). Furthermore, the director fluctuations, especially those with small wavevectors, should exhibit a somewhat slower relaxation. Using Eq. (4), we obtain the temperature dependence of the effective elastic constant K_{eff} , which has a similar temperature dependence as K_1 , which we have measured directly using the splay Frederiks transition in a planar cell [1,16,17], see Fig. 3(f). The presented analysis demonstrates that the temperature dependence of the elastic constants prevails over the temperature dependence of the dielectric anisotropy. This prevalence explains the observed temperature dependence of δn , Fig. 3(f).

The switching times τ_{on} and τ_{off} are almost independent of the applied electric field, Fig. 3(c), while their temperature dependences are different, Fig. 3(d). The monotonic increase of τ_{off} with temperature suggests that the ratio of a relevant viscous coefficient to the elastic constant is also increasing with temperature. This result is rather surprising, since the viscous coefficient usually decreases with temperature much faster than the elastic constants. A plausible explanation might be in the multicomponent nature of the material and nanosegregation effects that produce different spectra of the fluctuation modes at different temperatures; however, further studies are needed to understand the effect better. In contrast, the temperature dependence of τ_{on} exhibits a crossover: at high temperatures, above 44°C , τ_{on} remains almost constant, whereas below 44°C , τ_{on} increases upon cooling. The dielectric torque depends on both the present and past values of the electric field and the director when the rise time of the applied field is close to (or smaller than) the dielectric relaxation time [18,19]. This is the so-called dielectric memory effect. At low temperature, Debye relaxation is slower than the rise of the applied voltage, Fig. 1(b). Thus, we attribute the low temperature increase of τ_{on} to the temperature dependency of the Debye relaxation time τ_D , Fig. 1(b), and an associated memory effect in the field-induced polarization of the NLC. Figures 1(b) and 1(c) demonstrate that the Debye relaxation time is smaller than the pulse duration, and therefore, the memory effect [19] does not change the amplitude of the electro-optical response.

Since the MEMOP response time of approximately $10\ \mu\text{s}$ is significantly shorter than that of the response time of the conventional electro-optic Frederiks transition, the resulting figure of merit (FOM) equals $\delta\Gamma^2/\pi^2\tau_{\text{off}}$ of MEMOP is very high. In the Frederiks transition, a large τ_{off} represents the main bottleneck for applications. In the MEMOP effect, τ_{off} is practically the same as the field-on switching time τ_{on} . With the typical values measured in our work, $\delta n = 0.04$ and $\tau_{\text{off}} = 10\ \mu\text{s}$, and for a typical cell of thickness $d = 5\ \mu\text{m}$, one finds FOM approximately equals $10^2\ \mu\text{m}^2/\text{s}$. A typical Frederiks reorientation produces a weaker FOM of approximately $1\text{--}10\ \mu\text{m}^2/\text{s}$ [5]. Note here that the absolute limit of the induced birefringence in an NLC could not be higher than about $\delta n \sim 0.2$. The latter value corresponds to a perfect alignment of each and every molecule. However, the electric field required for creating such an idealistic perfectly aligned state with a maximum possible scalar order parameter $S = 1$ is much higher than the fields in our experiments. Consider, for example, a field with a dielectric extrapolation length that corresponds to a characteristic intermolecular distance a of a few nanometers. Such a field $E_c = \pi\sqrt{K_{\text{eff}}/\varepsilon_0\Delta\varepsilon}/a$ corresponds to the limit of the continuous elastic theory and is approximately $E_c \approx 200\ \text{V}/\mu\text{m}$ for $a \approx 2\ \text{nm}$. The latter value is one order of magnitude larger than the fields in our experiments. Note, however, that even with the field used in our work, one can easily achieve levels of $\delta\Gamma \geq \lambda/2$ for the field-induced optical retardance required for various electro-optical applications: With the typical $\delta n \approx 0.04$, the required condition $\delta\Gamma \geq \lambda/2$ is satisfied in cells of thickness $10\ \mu\text{m}$ and above.

IV. CONCLUSIONS

We demonstrate a MEMOP effect, a microsecond electro-optical response in the nematic material GPDA200 with an extraordinary high dielectric anisotropy $\Delta\varepsilon > +200$. The effect is mainly caused by the quenching of director fluctuations in the electric field that is applied parallel to the director. The field-induced birefringence in the range $0.01\text{--}0.04$ is produced by electric fields on the order of $10^7\ \text{V}/\mu\text{m}$. The described MEMOP effect yields a FOM one or two orders of magnitude higher than the conventional Frederiks effect. It is also of interest to compare the described MEMOP effect to the NEMOP effect observed in nematics with $\Delta\varepsilon < 0$ [10–12]. As compared to NEMOP, the MEMOP effect requires electric fields that are one order of magnitude lower to achieve a similar field-induced birefringence [12]. The tradeoff between NEMOP and MEMOP is in the response time versus the applied field. Although MEMOP is slower than NEMOP, its microsecond response times $\tau_{\text{on}} \approx \tau_{\text{off}} \approx 10\ \mu\text{s}$ are still very attractive for fast electro-optical applications. We conclude that the proposed MEMOP shows properties that

fill the gap between the conventional relatively slow Fredriks effects and the ultrafast nanosecond responses of NEMOP. As such, MEMOP is promising for a variety of applications in devices such as electrically controlled shutters and beamsteerers.

ACKNOWLEDGMENTS

We acknowledge useful discussions with Sathyanarayana Paladugu.

-
- [1] D.-K. Yang and S.-T. Wu, *Fundamentals of Liquid Crystal Devices* (John Wiley & Sons, Chichester, United Kingdom, 2014).
 - [2] B.-Y. Wei, W. Hu, Y. Ming, F. Xu, S. Rubin, J.-G. Wang, V. Chigrinov, and Y.-Q. Lu, Generating switchable and reconfigurable optical vortices via photopatterning of liquid crystals, *Adv. Mater.* **26**, 1590 (2014).
 - [3] L. Wang, Self-activating liquid crystal devices for smart laser protection, *Liq. Cryst.* **43**, 2062 (2016).
 - [4] A. Repiova and V. Frederiks, On the nature of the anisotropic liquid state of mater, *J. Russ. Phys. Chem. Soc.* **59**, 183 (1927).
 - [5] A. B. Golovin, S. V. Shiyanovskii, and O. D. Lavrentovich, Fast switching dual-frequency liquid crystal optical retarder, driven by an amplitude and frequency modulated voltage, *Appl. Phys. Lett.* **83**, 3864 (2003).
 - [6] X.-W. Lin, W. Hu, X.-K. Hu, X. Liang, Y. Chen, H.-Q. Cui, G. Zhu, J.-N. Li, V. Chigrinov, and Y.-Q. Lu, Fast response dual-frequency liquid crystal switch with photo-patterned alignments, *Opt. Lett.* **37**, 3627 (2012).
 - [7] W. Duan, P. Chen, B.-Y. Wei, S.-J. Ge, X. Liang, W. Hu, and Y.-Q. Lu, Fast-response and high-efficiency optical switch based on dual-frequency liquid crystal polarization grating, *Opt. Mater. Express* **6**, 597 (2016).
 - [8] W.-B. Jung, H. S. Jeong, H.-J. Jeon, Y. H. Kim, J. Y. Hwang, J.-H. Kim, and H.-T. Jung, Polymer-layer-free alignment for fast switching nematic liquid crystals by multifunctional nanostructured substrate, *Adv. Mater.* **27**, 6760 (2015).
 - [9] J.-W. Kim, T.-H. Choi, and T.-H. Yoon, Fast switching of nematic liquid crystals over a wide temperature range using a vertical bias electric field, *Appl. Opt.* **53**, 5856 (2014).
 - [10] V. Borshch, S. V. Shiyanovskii, and O. D. Lavrentovich, Nanosecond Electro-Optic Switching of a Liquid Crystal, *Phys. Rev. Lett.* **111**, 107802 (2013).
 - [11] V. Borshch, S. V. Shiyanovskii, B.-X. Li, and O. D. Lavrentovich, Nanosecond electro-optics of a nematic liquid crystal with negative dielectric anisotropy, *Phys. Rev. E* **90**, 062504 (2014).
 - [12] B.-X. Li, V. Borshch, S. V. Shiyanovskii, S.-B. Liu, and O. D. Lavrentovich, Electro-optic switching of dielectrically negative nematic through nanosecond electric modification of order parameter, *Appl. Phys. Lett.* **104**, 201105 (2014).
 - [13] B.-X. Li, S. V. Shiyanovskii, and O. D. Lavrentovich, Nanosecond switching of micrometer optical retardance by an electrically controlled nematic liquid crystal cell, *Opt. Express* **24**, 29477 (2016).
 - [14] B. Malraison, Y. Poggi, and E. Guyon, Nematic liquid crystals in high magnetic field: Quenching of the transverse fluctuations, *Phys. Rev. A* **21**, 1012 (1980).
 - [15] D. A. Dunmur, T. F. Waterworth, and P. Palfy-Muhoray, Electric field induced birefringence in nematic liquid crystal films: evidence for wall quenching of director fluctuations, *Mol. Cryst. Liq. Cryst.* **124**, 73 (1985).
 - [16] H. J. Deuling, Deformation of nematic liquid crystals in an electric field, *Mol. Cryst. Liq. Cryst.* **19**, 123 (1972).
 - [17] S.-T. Wu, C.-S. Hsu, and K.-F. Shyu, High birefringence and wide nematic range bis-tolane liquid crystals, *Appl. Phys. Lett.* **74**, 344 (1999).
 - [18] Y. Yin, S. V. Shiyanovskii, A. B. Golovin, and O. D. Lavrentovich, Dielectric Torque and Orientation Dynamics of Liquid Crystals with Dielectric Dispersion, *Phys. Rev. Lett.* **95**, 087801 (2005).
 - [19] S. V. Shiyanovskii and O. D. Lavrentovich, Dielectric relaxation and memory effects in nematic liquid crystals, *Liq. Cryst.* **37**, 737 (2010).